Histochem Cell Biol (2008) 130:681–692
DOI 10.1007/s00418-008-0448-1

ORIGINAL PAPER

Gold ions bio-released from metallic gold particles reduce inflammation and apoptosis and increase the regenerative responses in focal brain injury

Agnete Larsen · Kristian Kolind · Dan Sonne Pedersen · Peter Doering · Mie Østergaard Pedersen · Gorm Danscher · Milena Penkowa · Meredin Stoltenberg

Accepted: 13 May 2008 / Published online: 10 June 2008

Abstract Traumatic brain injury results in loss of neurons caused as much by the resulting neuroinflammation as by the injury. Gold salts are known to be immunosuppressive, but their use are limited by nephrotoxicity. However, as we have proven that implants of pure metallic gold release gold ions which do not spread in the body, but are taken up by cells near the implant, we hypothesize that metallic gold could reduce local neuroinflammation in a safe way. Bio-liberation, or dissolucytosis, of gold ions from metallic gold surfaces requires the presence of disolycytes i.e. macrophages and the process is limited by their number and activity. We injected 20–45 μm gold particles into the neocortex of mice before generating a cryo-injury. Comparing gold-treated and untreated cryolesions, the release of gold reduced microgliosis and neuronal apoptosis accompanied by a transient astrogliosis and an increased neural stem cell response. We conclude that bio-liberated gold ions possess pronounced anti-inflammatory and neuron-protective capacities in the brain and suggest that metallic gold has clinical potentials. Intra-cerebral application of metallic gold as a pharmaceutical source of gold ions represents a completely new medical concept that bypasses the blood-brain-barrier and allows direct drug delivery to inflamed brain tissue.

G. Danscher, M. Penkowa and M. Stoltenberg have contributed equally to the content of this manuscript.

A. Larsen (✉) · P. Doering · G. Danscher · M. Stoltenberg
Department of Neurobiology, Institute of Anatomy, University of Aarhus, 8000 Aarhus C, Denmark
e-mail: al@neuro.au.dk

K. Kolind · D. S. Pedersen · M. Ø. Pedersen · M. Penkowa
Section of Neuroprotection, the Panum Institute, University of Copenhagen, Copenhagen, Denmark

Keywords Apoptosis · Autometallography (AMG) · Dissolucytosis · Gold · Immunosuppression · Microglia · Neuroregeneration · Stem cells

Introduction

The inflammatory processes seen in the brain generally resembles the processes taking place in other tissues and the brain is thus no longer considered an immunologically privileged organ (Barker and Widner 2004). However, albeit important for brain tissue restoration, inflammatory processes in brain tissue inevitably result in tissue damage. An immune response in the brain is initiated by the microglia and the damaging effects of neuroinflammation are both immediate and include 'secondary delayed damage' caused by reactive oxygen species (Mhatre et al. 2004; Potashkin and Meredith 2006). In recent years it has become increasingly clear that neuroinflammation is also involved in the loss of neural tissue seen following stroke and traumatic brain injury as well as in the pathogenesis of neurodegenerative conditions like Alzheimer's disease (for details see Aktas et al. 2007).

Furthermore, autoimmune inflammation in the central nervous system plays a cardinal role in the pathogenesis of the most common neurodegenerative disease today, multiple sclerosis (MS). MS primarily affects young adults and at least 400,000 individuals suffer from MS in USA alone. In MS, microglia activated by auto-reactive T-cells cause a breakdown of the blood-brain-barrier, and the resulting invasion of various immune cells orchestrates a full-blown immune response.

The immuno-modulatory effects of gold ions have been used in the treatment of rheumatic arthritis for more than 50 years. Although the underlying mechanisms have never

been fully unraveled, it is known that gold ions alter the function of macrophages by inhibiting their lysosomal enzymes and lowering their production of pro-inflammatory cytokines (Persellin and Ziff 1966; Yanni et al. 1994). The use of gold compounds in medicine has however been limited due to adverse effects. Both parenterally and perorally administered gold compounds can cause pronounced nephrotoxicity and careful monitoring is needed when administering the traditional gold compounds (Tozman and Gottlieb 1987; Felson et al. 1990). These toxic effects can be by-passed by using local application of metallic gold particles/implants. Using autometallography (AMG) we have previously shown that gold ions are liberated from such implants in vivo and in vitro (Danscher 2002; Larsen et al. 2007). This bio-liberation, now termed dissolucytosis, is defined as the extracellular liberation of gold ions from the surface of gold particles bigger than 20 microns, i.e. particles that cannot be phagocytozed by macrophages. The process most likely involves a macrophage-induced reorganization of the biofilm which is created on the metallic surface immediately after an implant is placed in the organism (Sennerby et al. 1993; Futami et al. 2000; Larsen et al. 2007; Roach et al. 2007). This dissolution membrane makes it possible for the macrophages to control the chemical milieu at the gold surface and the dissolucytosis of gold ions is most likely caused by the capacity of the macrophages to manipulate releasing cyanide ions and altering the oxygen tension and the pH in their vicinity (Ferre and Claria 2006). The process of dissolucytosis is limited by (1) the size of the gold surface, (2) the amount of dissolucytotic macrophages, and their state of activity. The slow speed of the process results in limited liberation of gold ions taken up solely by cells close to the implant.

The present study focuses on the effects of bio-liberated gold ions on the inflammatory and reparatory responses taking place in brain tissue following a focal cryo-lesion.

Experimental procedures

Animals

Forty eight-week-old female C57b16 mice (Taconic M&B, Ry, Denmark) were used for this study. The animals were housed under standard conditions, i.e. a 12-h light/dark cycle at 22°C, and with free access to food and water. All experimental procedures were performed in accordance with Danish law.

The animals were divided into 2 groups each containing 20 animals. One group was intra-cranially injected with 2 × 2.72 mg metallic gold suspended in sodium hyaluronate just before cryo-lesioning (freeze-lesioning) the neocortex.

The animals in the other group served as controls and received only sodium hyaluronate injections before the brain injury.

Gold treatment

Ninety-nine per cent pure metallic gold (Alfa-Aesar, Ge) was sieved using 2 aluminum sieves (Retsch, Ge) to obtain gold particles in the size of 20–45 µm. 463 mg gold was mixed with 0.85 ml sodium hyaluronate (10 mg/ml, PROVISC, Alcon, Se) in a water bath set at 40°C.

Each animal was injected with a 2 × 5 µl gold-sodium hyaluronate mixture. Control animals were injected with 2 × 5 µl sodium hyaluronate. The injections were placed in the depth of the neocortex, 1 mm from the surface, at the following coordinates: 1 mm lateral, 1 mm posterior to Bregma and 1 mm lateral, 3 mm posterior to Bregma, respectively (Paxinos and Franklin 1997).

Prior to the injections, the animals were anesthetized with an injection of a mixture of Narcoxyl-vet (Xylazin) and Ketominal-vet. The deeply anesthetized animals were placed in a Benchmark stereotaxic instrument (myNeuroLab.com, USA) and a longitudinal incision was made in the skin covering the skull. Two drill holes were made under the microscope according to the Paxinos-Franklin coordinates, and the gold sodium hyaluronate/sodium hyaluronate injections were given in the centre of each drill hole.

Brain injury

Immediately after the injection of gold/sodium hyaluronate or sodium hyaluronate, respectively, a small pencil-shaped piece of dry ice was placed on the skull for 30 s The dry ice was placed exactly in the middle between the 2 drill holes.

This model of traumatic brain injury was previously described in details (Penkowa and Moos 1995; Penkowa et al. 1999, 2000, 2003). We have applied this freeze-lesion model for more than a decade producing very reliable (consistent and reproductive) results. In the present study, the model was modified as we shortened the freezing procedure (ice-skull contact) from 60 to 30 s in order to ensure animal survival after the combined stereotaxic injection and freeze-lesion.

After freeze-lesioning, the animals returned to their cages until 7 or 14 days post-lesion (dpl), after which they were deeply anesthetized with Mebumal (pentobarbital, 50 mg/ml, SAD, DK) and killed by decapitation or transcardial perfusion. A total of 20 animals, i.e., 10 gold exposed and 10 control animals were killed at each time point.

Autometallography (AMG)

The AMG developer consists of a 60 ml gum arabic solution (Bidinger, Aarhus, DK) and 10 ml sodium citrate buffer (23.5 g sodium citrate (Merck 6448, VWR, DK) to 100 ml distilled water), 15 ml reducing agent (0.85 g of hydroquinone (Merck 4610, VWR, DK) dissolved in 15 ml distilled water at 40°C), and 15 ml solution containing silver ions (0.12 g silver lactate (Fluka 85210 supplied by Sigma-Aldrich, Vallensbæk, DK) in 15 ml distilled water at 40°C); the latter is added immediately before use while thoroughly stirring the AMG solution.

The AMG development takes place in a water bath at 26°C for 60–70 min under a dark hood. Development is stopped by replacing the developer with a 5% thiosulphate solution for 10 min. Finally, the tissue sections/slices are rinsed several times in distilled water (for details see Danscher (1981) and Danscher and Stoltenberg (2006)).

Fixation and tissue processing for AMG

After transcardial perfusion with 3% glutaraldehyde (Merck 4239, VWR, Albertslund, DK) the mouse brain was immediately removed from the body and allowed to post-fixate in the same fixative for one hour.

Tissue slices to be analyzed in the light or electron microscope were treated in accordance with the following two procedures, respectively: (1) For light microscopical analyses the slices were placed in a 30% solution of sucrose until they sank to the bottom of the glass. The slices were then frozen with CO_2, placed in a cryostat, and allowed a temperature fall to −17ºC. After AMG development (see below), the sections were counterstained with a 0.1% solution of aqueous toluidine blue (pH 4.0), dehydrated in ascending concentrations of alcohol and xylene, embedded in DePex and covered with a cover glass. (2) For electron microscopy the slices were cut on a vibratome and the resulting 100-µm-thick sections were developed in AMG. The areas to be analyzed were cut out, placed in osmium tetroxide (1% in phosphate buffer for 30 min) and embedded in Epon. From these Epon blocks 3-µm-thick sections were cut and AMG developed. One of the three sections on each glass slide was counterstained with toluidine blue. After LM analysis, the sections to be analyzed further in the electron microscope were re-embedded on top of an Epon block. Ultrathin sections were cut, placed on a grid and counterstained with uranyl citrate and lead acetate (Danscher 1981; Danscher and Stoltenberg 2006).

Fixation and tissue processing for histopathological analyses

After decapitation, the brain was immediately removed and post-fixated for 2 days at room temperature in Zamboni's fixative (buffered 4% formaldehyde added 15% picric acid solution from a 1.2% saturated aqueous picric acid solution, pH 7.4).

All the fixed brains were processed for paraffin embedding in a fully automatic Shandon Excelsior Tissue Processor Histokinette. Afterwards, they were embedded in paraffin and cut in serial, coronal 7-µm-thick sections for histopathological analyses.

Sections embedded in paraffin were then re-hydrated according to standard procedures, after which they underwent heat-induced epitope retrieval (HIER) as earlier described in details by Penkowa et al. (2006). In short, HIER includes boiling in a microwave oven in citrate buffer, pH 9.1 or pH 6.0, for 10 min.

Sections were incubated in 1.5% H_2O_2 in Tris-buffered saline (TBS)/Nonidet (TBS: 0.05 M Tris, pH 7.4, 0.15 M NaCl; with 0.01% Nonidet P-40) (Sigma-Aldrich, USA, code N-6507) for 30 min at room temperature to quench endogenous peroxidase. Afterwards, the sections were incubated with 10% goat serum (In Vitro, DK, code 04009-1B) or donkey serum (The Binding Site, UK, code BP 005.1) in TBS/Nonidet for 30 min at room temperature in order to block nonspecific binding. Sections prepared for incubation with monoclonal mouse-derived antibodies were incubated with Blocking Solutions A + B from HistoMouse-SP Kit (Zymed Lab. Inc., USA, code 95-9544) to quench endogenous mouse IgG.

After these steps, the sections were ready for histochemistry, immunohistochemistry and detection of apoptosis by TUNEL.

Histochemistry

Sections were incubated overnight at 4°C with biotinylated tomato lectin from *Lycopersicon esculentum* (Sigma-Aldrich, USA, code L9389) 1:500, which was used as a marker for myelo-monocytic cell types, such as all microglial populations (e.g. ramified, resident microglia, perivascular microglia, and round activated microglial macrophages as identified by morphological examination),hematogenous monocytes and macrophages as well as the tomato lectin stained vascular endothelium (Acarin et al. 1994; Santos et al. 2008).

The lectin was developed using streptavidin-biotin-peroxidase complex (StreptABComplex/HRP, Dako, DK, code K377), prepared according to the manufacturer's

recommended dilutions, for 30 min at room temperature. The lectin staining was visualized using 0.015% H_2O_2 in 3, 3-diaminobenzidine-tetrahydrochloride (DAB)/TBS for 10 min at room temperature.

Immunohistochemistry

The immunohistochemical procedures applied were previously described in detail (Futami et al. 2000; Gage 2000; Gilbertson and Rich 2007; Ihrie and Alvarez-Buylla 2008).

The sections were incubated overnight at 4°C with the following primary antibodies: Rabbit anti-GFAP (a marker of astrocytes) diluted 1:250 (Dako, DK, cat. no.: Z334); Rabbit anti-frizzled-9 (a marker of neural stem cells) diluted 1:100 (AbCam, USA, cat. no.: ab13000).

The primary antibodies were detected using biotinylated secondary antibodies (incubation for 30 min at room temperature) as previously described and listed in Penkowa et al. (1999, 2000, 2003, 2004, 2006), followed by streptavidin-biotin-peroxidase complexing (StreptABComplex/HRP, Dako, DK, code K377) and tyramide signal amplification (TSA)-kit (NEN, Life Science Products, USA, code NEL700A), according to the manufacturer's recommendations. Finally, the immunoreactions were visualized using DAB as chromogen.

In all experiments, the extent of non-specific binding of the antisera was evaluated by omitting the primary antibody step. Results were considered only if these controls were negative.

In situ detection of DNA fragmentation (TUNEL)

Terminal deoxynucleotidyl transferase (TdT)-mediated deoxyuridine triphosphate (dUTP)-biotin nick end labeling (TUNEL) was performed using the Fragment End Labeling (FragEL) Detection Kit (Calbiochem, USA, code QIA33). The FragEL kit contains all the materials used below and each step was performed according to the manufacturer's recommendations. Rehydrated sections were incubated with 20 µg/ml proteinase K for 20 min to strip off nuclear proteins. After immersion in equilibration buffer for 20 min, the sections were incubated with TdT and biotin-labeled deoxynucleotids (dNTP-biotin) in a humified chamber at 37°C for 1.5 h. This was followed by a wash buffer and the stop solution for 5 min at room temperature to stop the reaction. After washing in TBS and incubation in blocking buffer for 10 min, the sections were incubated with peroxidase-streptavidin for 30 min and afterwards DAB was used as chromogen. The sections were counterstained with methyl-green. Negative control sections were treated similarly, but incubated in the absence of TdT enzyme or dNTP-biotin or peroxidase-streptavidin.

Detection of in situ apoptosis

TUNEL stained tissue sections were compared with positive control slides provided in the FragEL Detection Kit as well as with tissue sections stained for the apoptotic markers p53 and activated caspase-3. In addition, morphologic criteria for apoptosis (e.g. cell shrinkage, formation of apoptotic bodies, membrane blebbing, pyknotic nuclei) were evaluated. The degree of neuronal apoptosis was evaluated by fluorescence labeling.

Fluorescence labeling

In order to substantiate if neurons suffer from apoptosis, double staining for TUNEL and neuronal cells was carried out. Hence, TUNEL was performed only omitting the DAB chromogen followed by incubation at 4°C with rabbit anti-human NSE diluted 1:1,000 (Calbiochem, USA, cat. no.: D05059). The anti-NSE antibodies were detected by using goat anti-rabbit IgG linked with TexasRed (TXRD) diluted 1:40 (Jackson ImmunoResearch Lab. Inc., cat.no.: 111-075-144), and TUNEL was visualized by using aminomethylcoumarin (AMCA)-linked TSA-kit (NEN, Life Science Products, USA, cat.no.: NEL703) as recommended by the manufacturer.

For the simultaneous examination and recording of the three stains, a Zeiss Axioplan2 light microscope equipped with a tripleband (FITC/TXRD/AMCA) filter was used.

Cell counts and statistical analysis

In addition to morphological evaluation, counting of the variables analyzed was carried out.

Quantifications were made after the brain injury in 0.5 mm^2 matched area of the 7 µm brain sections at the border of the cortical lesion (the rim between lesioned and unlesioned brain tissue) as depicted in the photomicrographs.

For each parameter analyzed, brain sections from at least 3 mice ($n = 3–5$) of each group were used and a mean value of the positively stained cells was calculated.

Positively stained cells were defined as cells with positive staining of the soma except in the case of TUNEL staining of apoptotic cells where the apoptotic cells were defined as those with nuclear staining (nuclear TUNEL).

The cell counts were performed by the same investigator, who was blinded to the animal identity and the treatments. The quantifications were used for statistical comparisons of the gold treatment versus the placebo effect upon the neurobiological responses to a brain injury. For statistical group comparisons, Student's *t*-test was used. As the five parameters tested are unlikely to be independent, corrections for mass significance were not applied.

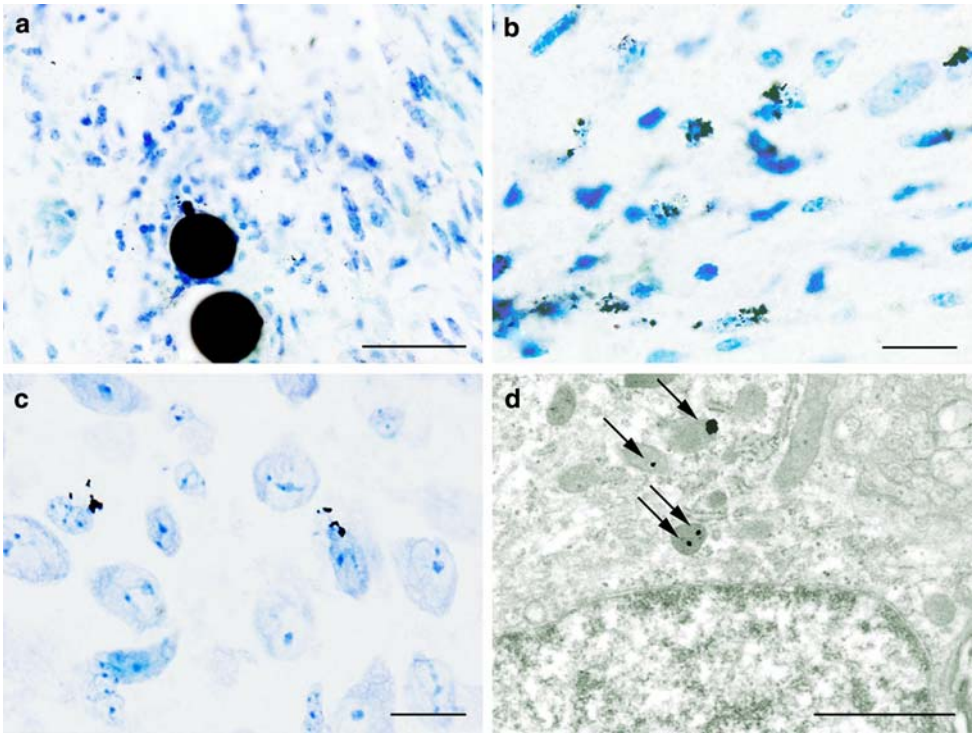

Fig. 1 Micrographs showing gold implants and adjacent gold uptake in AMG developed tissue, 14 dpl. **a** 30-µm-thick cryo section showing two silver enhanced gold implants placed in the neuroinflammatory area. Gold loaded cells in the vicinity of the implants can be seen. *Scale bar*: 50 µm. **b**, **c** High magnification micrographs visualizing cellular uptake of silver enhanced gold ions. Semithin 5 µm section. *Scale bars*: 15 µm. **d** Electron micrograph of AMG silver enhanced gold ions exclusively located in lysosomes (*arrows*). *Scale bar*: 1 µm

Results

Gold tracing

Light microanalysis of AMG developed sections showed fine traces of liberated gold ions in tissue near the gold deposit within the region of the lesion and its border zone. In this area, cytoplasmatic accumulation of silver enhanced nanogold particles was seen in both glia cells and neurons (Fig. 1a–c). At ultrastructural levels the AMG enhanced nanogold particles were found to be located in lysosome-like organelles (Fig. 1d). The number of gold labeled lysosomes was sparse as was the amount of AMG grains in each lysosome (Fig. 1d). All control sections were void of AMG staining.

Anti-inflammatory effects

The bio-liberation of gold had a marked impact on the inflammatory responses to the cryo-lesion resulting in an increased GFAP activity in the early phase, 7 days after the lesion (Figs. 2a, 3), along with a long-lasting reduction of the number of microglia/macrophages (Fig. 4). The reduction was observed as a lowering of the number of activated, round macrophages at both the early (7 days) and the late phase (14 days) (Fig. 2b). A statistically significant reduction in the amount of resting, ramified macrophages was seen after 14 days (Fig. 2c) while only a slightly reduced number of resting macrophages was recorded at day 7.

Neuroprotective and regeneratory effects

Gold-induced neuroprotection in terms of reduced apoptotic cell death, i.e. number of cells with nuclear TUNEL stain, was seen both in the early and the late phase (Figs. 2d, 5a–d) and double-staining combining NSE and TUNEL confirmed that the gold treatment could circumvent apoptosis in neurons (Fig. 5e, f).

The dissolucytotically liberated gold ions were also found to increase the number of frizzled-9 positive neural stem cells present at both time points (Figs. 2e, 6) as compared to the stem cell responses seen in the control lesioned mice. As seen in Fig. 6g–h, both the mitosis of stem cells at the subventricular zone (SVZ) (Fig. 6c–f) and stem cell migration towards the lesion cavity (Fig. 6g–h) were up-regulated by the gold treatment.

Mean and SEM values of all cell counting procedures are graphically illustrated in Fig. 2.

Discussion

This study is the first to show that metallic gold suppresses inflammation in the brain. Our previous finding that bio-released gold ions accumulate in glia and neurons of normal rats (Danscher 2002) and the present convincing data proving that gold ions process anti-inflammatory qualities towards immune reactions in the CNS lead us to believe that gold ions released in areas of neuroinflammation would

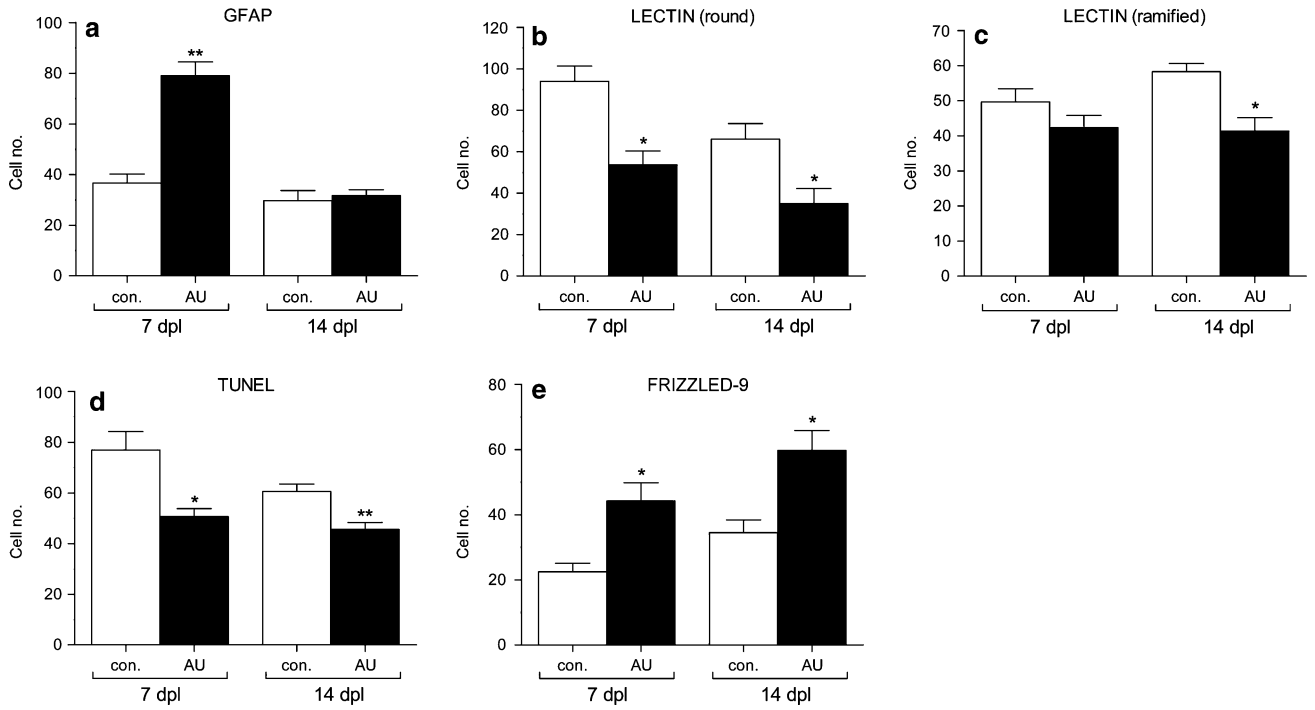

Fig. 2 Bar histograms depicting the brain tissue responses (cell counts, mean + SEM) seen 7 and 14 days after freeze-lesioning with AU or without (control) simultaneous gold-sodium hyaluronate injection. Statistically significant differences are indicated by * ($2P < 0.05$) and ** ($2P < 0.01$). **a** GFAP stained astroglia. Mean values at 7 dpl: 36.67 in the control group versus 79.00 in the gold treated group ($n = 3$, $2P = 0.0029$) Mean values at 14 dpl: 29.67 in the control group versus 31.67 in the gold treated group ($n = 3$, $2P = 0.6910$). **b** Lectin stained round (activated) macrophages. Mean values at 7 dpl 94.00 in the control group versus 53.67 in the gold treated group ($n = 3$, $2P = 0.0156$). Mean values at 14 dpl 66.00 in the control group versus 35.00 in the gold treated group ($n = 3$, $2P = 0.0414$). **c** Lectin stained ramified (resting) macrophages. Mean values at 7 dpl 49.67 in the control group versus 42.33 in the gold treated group ($n = 3$, $2P = 0.2254$). Mean values at 14 dpl 58.33 in the control group versus 41.33 in the gold treated group ($n = 3$, $2P = 0.0194$). **d** TUNEL + stained (nuclear stain) cells. Mean values at 7 dpl 77.00 in the control group versus 50.67 in the gold treated group ($n = 3$, $2P = 0.029$). Mean values at 14 dpl 60.60 in the control group versus 45.60 in the gold treated group ($n = 5$, $2P = 0.0061$). **e** FRIZZLED-9 stained stem cells. Mean values at 7 dpl 22.50 in the control group versus 44.25 in the gold treated group ($n = 4$, $2P = 0.0126$). Mean values at 14 dpl 34.5 in the control group versus 59.75 in the gold treated group ($n = 4$, $2P = 0.0133$)

dampen the process. Our results stress the potential of using gold particles as a way of reducing or even stop immunological abnormalities in the CNS. The weight of the 20–45 μm gold particles injected per animal was as little as 5.4 mg and the actual liberation of gold ions so sparse that it will be extremely difficult or impossible to measure. The accumulated gold crystals are but a few nanometers in diameter and can be made visible only because of the extremely sensitive autometallographic technique (Danscher 1981; Danscher and Stoltenberg 2006). The primary target of the liberated gold ions was the dissolucytotic macrophage/microglia population, and we saw a dramatic decline in the number of activated macrophage/microglia in the gold treated animals compared to the macrophage/microglia response seen following the control lesions (57% at day 7, 47% at day 14). This finding probably reflects a reduced recruitment of blood-borne macrophages. Reduction in the number of synovial macrophages is a known effect of conventional gold treatment of rheumatoid arthritis (Yanni et al. 1994), accompanied by a reduced production of pro-inflammatory cytokines such as IL-1α, IL-1β and TNF-α (Chang et al. 1990; Yanni et al. 1994; Bondeson and Sundler 1995). Our findings most likely mimic the events seen in connective tissues, i.e. a gold-induced alteration in the cytokine secretion from macrophages/microglia that in turn influences the recruitment and the activation of this cell population. Down-regulation of vascular cell adhesion molecules might also contribute to the anti-inflammatory effects of the bio-released gold ions as such effects are known from studies on gold sodium thiomalate (Koike et al. 1994).

Activated microglia/macrophages contribute to neurodegeneration and apoptosis through their production of cytotoxic reagents like reactive oxygen/nitrogen intermediates, proteolytic enzymes and proinflammatory cytokines (Block et al. 2007; Dheen et al. 2007). The emergence of inflammatory infiltrates is part of the pathology in a wide range of neurodegenerative diseases such as Alzheimer's disease, Parkinson's disease, and multiple sclerosis, although microglia/macrophages have also been shown to limit

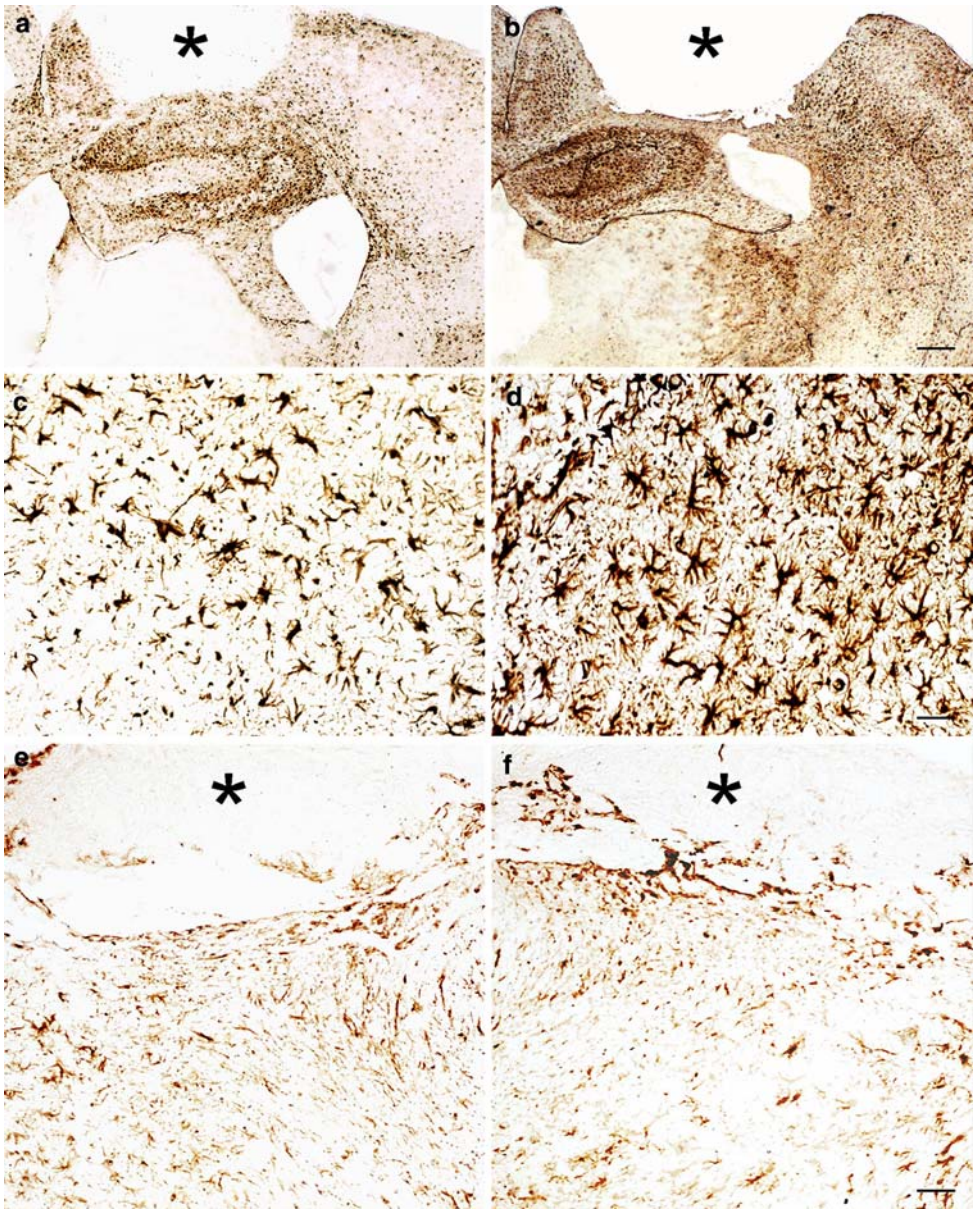

Fig. 3 GFAP immunostainings in lesioned mice at 7 (**a**–**d**) and 14 (**e**–**f**) dpl. **a** At 7 dpl, placebo-treated mice showed reactive astrogliosis in the ipsilateral hemisphere, while some reactive astrocytes were also seen in the contralateral cortex. The reactive astrocytes were situated around the lesion cavity (*asterisk*). **b** Increased reactive astrogliosis was seen in both hemispheres of the gold-treated mice at 7. dpl. **c** Higher magnification of **a**. **d** Higher magnification of **b**. **e**–**f** At 14 dpl, mice treated with placebo (**e**) and gold (**f**) showed a lesion (*asterisk*) surrounded by GFAP + reactive astrocytes. *Scale bars*: **a**, **b** = 228 μm; **c**, **d** = 27 μm; **e**, **f** = 42 μm

neuronal injury under certain biological conditions (Turrin and Rivest 2006). Accordingly, the reduced microgliosis is likely to contribute to the neuroprotective effects of the gold treatment, i.e. the marked reduction in the number of apoptotic neurons (Fig. 5e, f) seen in this study. The fact that the injury-induced apoptosis is seen mainly among neurons supports the theory that the reduced microgliosis is not due to increased microglial cell death, but results from an altered macrophage activity/cytokine secretion.

In addition to effects on the microglia/macrophage cell population gold treated animals exhibited statistically significantly increased astrogliosis. This finding is somewhat paradoxical as inflammation generally induces astrogliosis and further studies into the mechanisms by which gold liberation causes this response is warranted. Reactive astrocytes are considered as main source of neuroprotective factors including anti-inflammatory-, antioxidant- and anti-apoptotic mediators in the brain, and astroglia are critical for neuronal survival and functioning (Aschner et al. 2002; Penkowa et al. 2004; Sofroniew 2005; Seifert et al. 2006). Moreover, astrocytic cells give rise to multipotent neural stem cells and ongoing neurogenesis in the adult brain (Morshead et al. 2003; Myers et al. 2006; Vaccarino et al. 2007). Astrocytes are thus important targets for neuroprotective and regenerative interventions, and astrogliosis may partly explain the observed neuroprotective effects of the bio-liberated gold ions. Like other heavy metals, gold ions can induce metallothioneins (Sharma and McQueen 1981; Mogilnicka and Webb 1982), hereby working synergistically with the other neuroprotective effects of the transient astrogliosis.

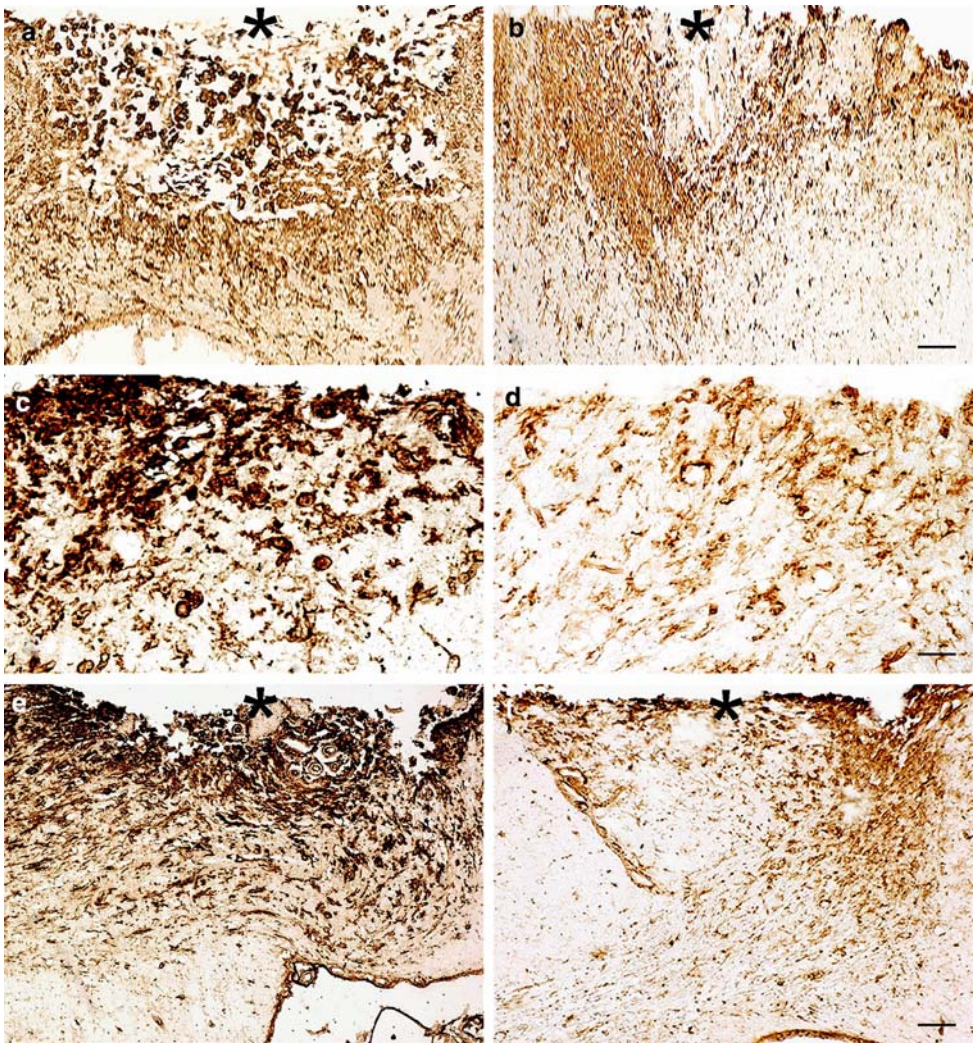

Fig. 4 Lectin stainings in lesioned mice at 7 (**a**–**d**) and 14 (**e**–**f**) dpl. **a** At 7 dpl, placebo-treated mice showed numerous lectin + macrophages/activated microglia in the injured cortex, where macrophages infiltrated the lesioned necrotic tissue (*asterisk*). **b** Decreased activation of macrophages/activated microglia was seen at the lesion site (*asterisk*) in gold-treated mice at 7 dpl. **c** Higher magnification of **a**. **d** Higher magnification of **b**. **e** At 14 dpl, macrophages/activated microglia were still found at the lesion site (*asterisk*) of mice treated with placebo. **f** Gold-treated mice had fewer lectin + macrophages/microglia in the lesioned cortex at 14 dpl. *Scale bars*: **a**, **b** = 34 μm; **c**, **d** = 20 μm; **e**, **f** = 26 μm

Generation of mature neurons were long believed to take place only during embryonic development, it has, however, now been established that a pool of neural stem cells still exists in the adult brain (Alvarez-Buylla et al. 2001, Simard and Rivest 2004; Ihrie and Alvarez-Buylla 2008). Frizzel-9 is a specific marker of these neural progenitors of astrocytic linage (Van Raay et al. 2001, Cai et al. 2002) which are capable of differentiating into both astrocytes, oligodendrocytes and neurons. The neural progenitors can be found throughout life in a few restricted areas of the CNS, i.e. the subventricular zone (SVZ) near the lateral ventricle and the subgranular zone (SGZ) in the hippocampus (Gage 2000; Simard and Rivest 2004; Ihrie and Alvarez-Buylla 2008) and it is well-known that injury induces increased neurogenesis within these areas (Parent 2003; Zhang et al. 2005; Okano et al. 2007).Inflammation has a high impact on adult neurogenesis (for a review see Das and Basu 2008), we cannot, however, fully explain why the presence of bio-liberated gold ions enhances he proliferation of frizzled-9-positive cells at the SVZ. Activated microglia have been shown to reduce neurogenesis (Ekdahl et al. 2003; Monje et al. 2003) whereas quiescent ones have the opposite effect (Monje et al. 2003; Walton et al. 2006). On the other hand, Butovsky and co-workers have shown that IFN-γ stimulation can create a population of activated microglia capable of inducing neurogensis (Butovsky et al. 2005, 2006). Apparently, gold ions not only increased the generation of neural progenitors but also facilitated the migration of neural cells to the injured brain area (Fig. 6a–h). This observation is most evident at day 14 after the lesion, at which time point neural progenitors i.e. frizzled-9 positive cells of stem cell morphology can be found near the lesion in the gold treated animals whereas such cells are barely seen (Fig. 6g, h) in this area in the control group. A few frizzled-9 postive vessels can also be seen at this time, corresponding well with studies of brain tumors in which co-localization of neurnal stem cell markers and vascular markers have been reported (Gilbertson and Rich 2007; Kang et al. 2008). The presence of frizzeled-9 positive cells in brain tumours is not surprising as tumour stem cells are known to be recruited

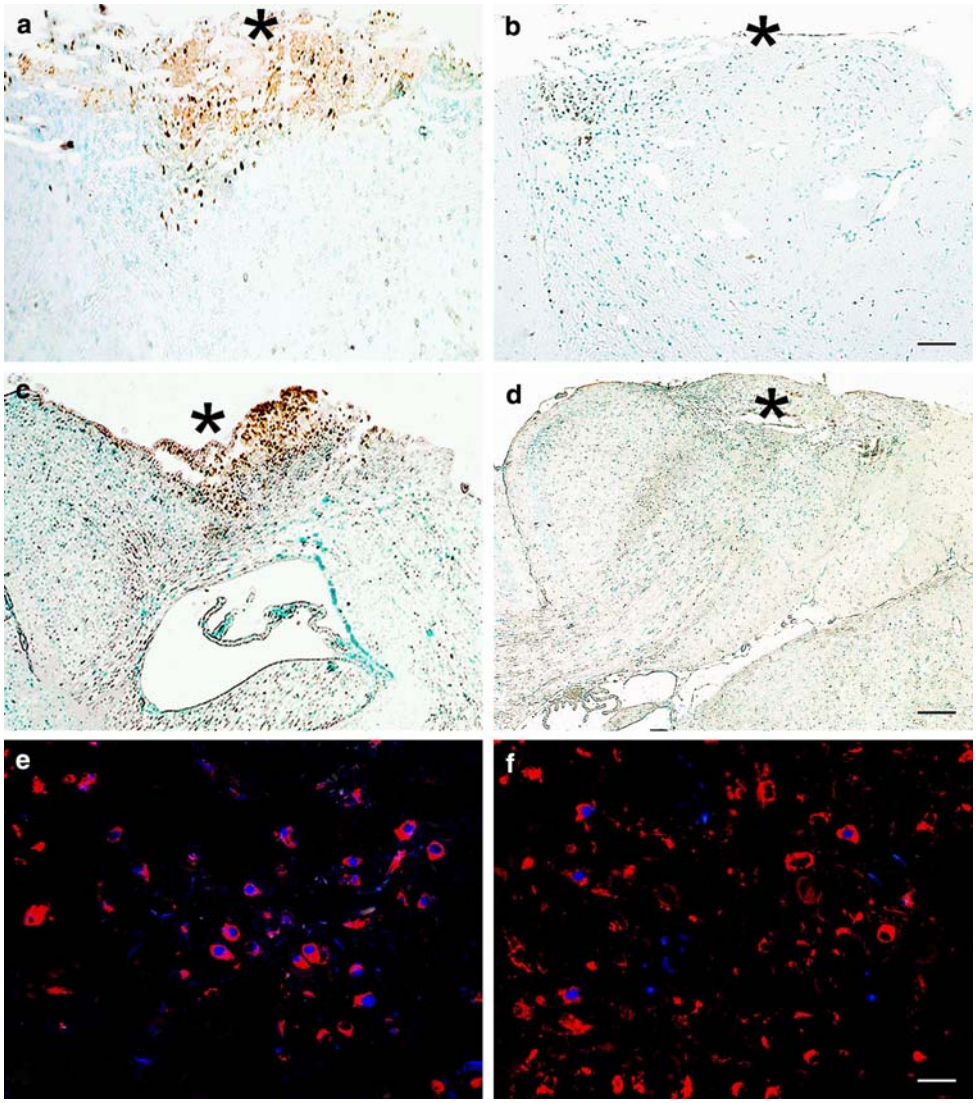

Fig. 5 TUNEL and co-localization by fluorescence in lesioned mice at 7 (**a**, **b**, **e**, **f**) and 14 (**c**, **d**) dpl. **a** Placebo-treated mice showed several TUNEL + cells in the lesioned area (*asterisk*) at 7 dpl. **b** TUNEL + cells were clearly reduced in the lesioned cortex of gold-treated mice at 7 dpl. **c**, **d** Cells stained by TUNEL were still plentiful at 14 dpl in the placebo group (**c**), while gold treatment (**d**) reduced cell death. **e**, **f** Double stainings for NSE + neurons (TXRD, *red*) and TUNEL (AMCA, *blue*). In mice treated with placebo (**e**), the neurons are the main cerebral cell type suffering from apoptosis. The gold-treated mice (**f**) displayed fewer apoptotic neurons. *Scale bars*: **a**, **b** = 53 μm; **c**, **d** = 88 μm; **e**, **f** = 25 μm

both from astrocytes and from haematogenous stem cells from the bone marrow. Additionally, a massive endothelial proliferation including their bone-marrow derivated progenitors are seen in brain tumours and astrocytes/astrocytomas do themselves produces a lot of both angiogene and stem-cell promoting factors and the presence of stem cell/progenitor properties in various cells types such as blood vessels are thus not unusual (Batchelor et al. 2007; Gilbertson and Rich 2007; Kang et al. 2008).

The increased amount of neural progenitor cells seen in the gold-treated animals in this study indicate that it is worthwhile to further explore the therapeutic properties of metallic gold particles, not only in relation to their anti-inflammatory properties per see, but also as a possible remedy for neuroprotection and increased neuroregeneration.

A safe local gold cure can be obtained by using even very small (>20 μm and thus non-phagocytosable) gold particles/implants, hereby limiting any damaging effects of the implantation itself, and investigations in our laboratory indicate that placing gold particles/implants within the ventricular system could be a feasible way to circumvent placing the metal directly in the brain tissue. The amount of gold ions liberated through dissolucytosis is so limited and localized that even micron-meter sized implants could serve as a lifelong cure with a minimal risk of toxic side effects. The increased number and activity of microglia/macrophages during an ongoing inflammation will automatically increase the amount of gold liberated when it is most needed.

In conclusion: Bio-liberated gold ions reduce microgliosis and apoptotic neuronal dead and increase the neuroregeneratory responses following a focal brain injury.

The effect on macrophages/microglia indicates that gold liberation treatment is an approach with clinical dimensions for ameliorating neuroinflammation. Furthermore, such treatment seems to have both neuroprotective and neuroregenerative potential.

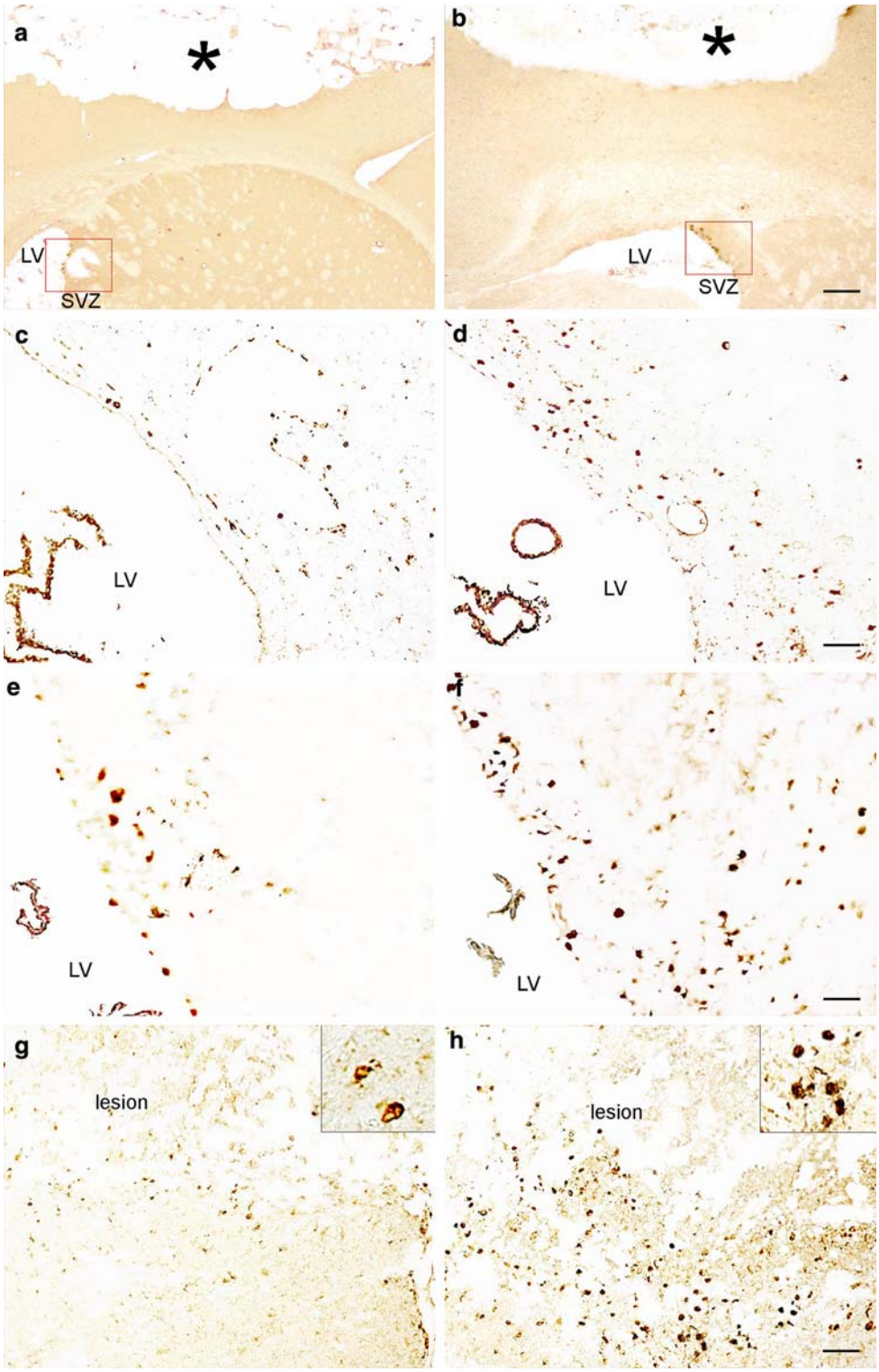

Fig. 6 Frizzled-9 immunostainings in lesioned mice at 7 (**a**–**d**) and 14 (**e**–**h**) dpl. **a**, **b** Low powered magnification showing brains of placebo (**a**) and gold (**b**) treated mice at 7 dpl. The photos show the lesioned cortex (*asterisk*) and the part of the lateral ventricles (LV) containing the subventricular zone (SVZ), where the neural stem cells (NSC) are generated. **c** Higher magnification of the framed area in **a**, which shows frizzled-9 + cells in the SVZ (adjacent to the LV) of placebo-treated mice. **d** Higher magnification of **b** showing the LV and SVZ of gold-treated mice. In both groups, NSCs are found in and adjacent to the SVZ at 7 dpl. **e**, **f** In the SVZ at 14 dpl, many NSCs were detected in animals receiving placebo (**e**) and/or gold (**f**). **g**, **h** At 14 dpl, frizzled-9 + cells could be detected in the tissue surrounding the lesion cavity, which indicates the presence of SVZ-derived frizzled-9 + cells in the lesioned cortex. Although NSCs were detected in both treatment groups, the frizzled-9 + cells were more prominent in gold-treated mice relative to placebo groups. This difference was most obvious in the cerebral cortex at 14 dpl. *Scale bars*: **a**, **b** = 130 μm; **c**, **d**, **g**, **h** = 54 μm; **e**, **f** = 32 μm

Acknowledgments The authors are grateful for the skillful technical assistance of Magdalena Maria Kus, Dorete Jensen, Albert Meier, Majken Sand and Karin Wiedemann. We gratefully acknowledge the financial support from the following foundations: IMK Almene Fond, Aase and Ejnar Danielsens Fond, Hede Nielsen Fonden, Fonden til Lægevidenskabens Fremme, Eva & Henry Frænkels Mindefond, Dir. Leo Nielsens Legat, Kathrine og Vigo Skovgaards Fond, Th. Maigaard's Efttf. Fru Lily Benthine Lunds Fond af 1/6 1978, and the Aarhus University Research Foundation.

Conflicts of interest Professor Danscher owns a small company, Berlock ApS, supported by government money that have patented the use of heavy metals as a dispenser of metal ions: European Patent: EP 1 395 268 (issued on January 19, 2005)based on the article "In vivo

liberation of gold ions from gold implants. Histochem Cell Biol (2002) 117:447–452. The present study has been carried out at the two university laboratories (University of Aarhus and University of Copenhagen, Denmark) named in the article and the company has not been involved in the work in any way.

References

Acarin L, Vela JM, Gonzkez B, Castella B (1994) Demonstration of poly-N-acetyl lactosamine residues in ameboid and ramified microglial cells in rat brain by tomato lectin binding. J Histochem Cytochem 42:1033–1041

Alvarez-Buylla A, García-Verdugo JM, Tramontin AD (2001) A unified hypothesis on the lineage of neural stem cells. Nat Rev Neurosci 2:287–293

Aktas O, Ullrich O, Infante-Duarte C, Nitsch R, Zipp F (2007) Neuronal damage in brain inflammation. Arch Neurol 64:185–189

Aschner M, Sonnewald U, Tan KH (2002) Astrocyte modulation of neurotoxicity. Brain Pathol 12:475–481

Barker RA, Widner H (2004) Immune problems in central nervous system cell therapy. Neurox 1:472–482

Batchelor TT, Sorensen AG, di Tomaso E, Zhang WT, Duda DG, Cohen KS, Kozak KR, Cahill DP, Chen PJ, Zhu M, Ancukiewicz M, Mrugala MM, Plotkin S, Drappatz JT, Louis DN, Ivy P, Scaddden DT, Benner T, Wen Loefller JS, PY Jain RK (2007) AZD2171, a pan-VEGF receptor tyrosine kinase inhibitor. normalizes tumor vasculature and alleviates edema in glioblastoma patients. Cancer Cell 11:83–95

Block ML, Zecca L, Hong JS (2007) Microglia-mediated neurotoxicity: uncovering the molecular mechanisms. Nat Rev Neurosci 8:57–69

Bondeson J, Sundler R (1995) Auranofin inhibits the induction of interleukin 1 beta and tumor necrosis factor alpha mRNA in macrophages. Biochem Pharmacol 50:1753–1759

Butovsky O, Talpalar AE, Ben-Yaakov K, Schwartz M (2005) Activation of microglia by aggregated beta-amyloid or lipopolysaccharide impairs MHC-II expression and renders them cytotoxic whereas IFN-gamma and IL-4 render them protective. Mol Cell Neurosci 29:381–393

Butovsky O, Ziv Y, Schwartz A, Landa G, Talpalar AE, Pluchino S, Martino G, Schwartz M (2006) Microglia activated by IL-4 or IFN-gamma differentially induce neurogenesis and oligodendrogenesis from adult stem/progenitor cells. Mol Cell Neurosci 31:149–160

Cai J, Wu Y, Mirua T, Pierce JL, Lucero MT, Albertine KH, Spangrude GJ, Rao MS (2002) Properties of a fetal multipotent neural stem cell (NEP Cell). Dev Biol 251:221–240

Chang DM, Baptiste P, Schur PH (1990) The effect of antirheumatic drugs on interleukin (IL-1) activity and IL-1 and IL-1 inhibitor production by human monocytes. J Rheumatol 17:1148–1157

Das S, Basu A (2008) Inflammation: a new candidate in modulating adult neurogenesis. J Neurosci Res 86(6):1199–1208

Danscher G (1981) Localization of gold in biological tissue. A photochemical method for light and electron microscopy. Histochemistry 71:81–88

Danscher G (2002) In vivo liberation of gold ions from gold implants. Autometallographic tracing of gold in cells adjacent to metallic gold. Histochem Cell Biol 117:447–452

Danscher G, Stoltenberg M (2006) Autometallography (AMG) Silver enhancement of quantum dots resulting from (1) metabolism of toxic metals in animals and humans, (2) in vivo, in vitro and immersion created zinc-sulphur/zinc-selenium nanocrystals, (3) metal ions liberated from metal implants and particles. Prog Histochem Cytochem 41:57–139

Dheen ST, Kaur C, Ling EA (2007) Microglia activation and its implications in brain diseases. Curr Med Chem 14:1189–1197

Ekdahl CT, Claasen JH, Bonde S, Kokaia Z, Lindvall O (2003) Inflammation is detrimental for neurogenesis in adult brain. Proc Natl Acad Sci USA 100:13632–13637

Felson DT, Anderson JJ, Meenan RF (1990) The comparative efficacy and toxicity of second-line drugs in rheumatoid arthritis. Results of two metaanalyses. Arthritis Rheum 34:1342–1343

Ferre N, Claria J (2006) New insight into the regulation of liver inflammation and oxidative stress. Mini Rev Med Chem 6:1321–1330

Futami T, Ohnishi H, Taguchi N, Kusakari H, Oshima H, Maeda T (2000) Tissue response to titanium implants in the rat maxilla: ultrastructural and histochemical observations of the bone-titanium interface. J Periodontol 71:287–298

Gage FH (2000) Mammalian neural stem cells. Science 287:1433–1438

Gilbertson RJ, Rich JW (2007) Making a tumour's bed: glioblastoma stem cells and the vascular niche. Nat Rev Cancer 7:733–736

Ihrie RA, Alvarez-Buylla A (2008) Cells in the astroglial lineage are neural stem cells. Cell Tissue Res 331:179–191

Kang MK, Hur BI KOMH, Kim CH, Cha SH, Kang SK (2008) Potential identity of multi-potential cancer stem-like subpopulation after radiation of cultured brain glioma. BMC Neurosci 9:15

Koike R, Miki I, Otoshi M, Totsuki T, Inoue H, Kase H, Saito I, Miyasuka N (1994) Gold sodium thiomalate down-regulates intercellular adhesion molecule-1 and vascular cell adhesion molecule-1 expression on vascular endothelial cells. Mol Pharmacol 46:599–604

Larsen A, Stoltenberg M, Danscher G (2007) In vitro liberation of charged gold atoms. Autometallographic tracing of gold ions released by macrophages grown on metallic gold surfaces. Histochem Cell Biol 128:1–6

Mhatre M, Floyd RA, Hensley K (2004) Oxidative stress and neuroinflammation in Alzheimer's disease and amylotrophic lateral sclerosis: common links and potential therapeutic targets. J Alzheimer Dis 6:147–157

Mogilnicka E, Webb M (1982) Comparative studies on the distribution of gold, copper and zinc in the livers and kidneys of rats and hamsters after treatment with sodium [195Au]-aurothiomalate. Chem Biol Interact 40:247–256

Monje ML, Toda H, Palmer TD (2003) Inflammatory blockade restores adult hippocampal neurogenesis. Science 302:1760–1765

Morshead CM, Garcia AD, Sofroniew MV, Der Kooy D (2003) The ablation of glial fibrillary acidic protein-positive cells from the adult central nervous system results in the loss of forebrain neural stem cells but not retinal stem cells. Eur J NeuroSci 18:76–84

Myers D, Gurkoff GG, Lee GM, Hovda DA, Sofroniew MV (2006) Essential protective roles of reactive astrocytes in traumatic brain injury. Brain 129:2761–2772

Okano H, Sakaguchi M, Ohki K, Suzuki N, Sawamoto K (2007) Regeneration of the central nervous system using endogenous repair mechanisms. J Neurochem 102:1459–1465

Parent JM (2003) Injury-induced neurogenesis in the adult mammalian brain. Neuroscientist 9:261–272

Paxinos G, Franklin KBJ (1997) The mouse brain in stereotaxic coordinates, 2nd edn. Elsevier Science, USA

Penkowa M, Moos T (1995) Disruption of the blood-brain interface in neonatal rat neocortex induces a transient expression of metallothionein in reactive astrocytes. Glia 13:217–227

Penkowa M, Moos T, Carrasco J, Hadberg H, Molinero A, Bluethmann H, Hidalog J (1999) Strongly compromised inflammatory response to brain injury in interleukin-6 deficient mice. Glia 25:343–357

Penkowa M, Giralt M, Carrasco J, Hadberg H, Hidalgo J (2000) Impaired inflammatory response and increased oxidative stress and neurodegeneration after brain injury in interleukin-6-deficient mice. Glia 32:271–285

Penkowa M, Camats S, Hadberg H, Quintana A, Rojos S, Giralt M, Molinero A, Campelll IL, Hidalogo J (2003) Astrocyte-targeted expression of IL-6 protects the CNS against a focal brain injury. Exp Neurol 181:130–148

Penkowa M, Quintanta A, Carrasco J, Giralt M, Molinero A, Hidalgo J (2004) Methallothionein prevents neurodegeneration and central nervous system. J Neurosci Res 77:35–53

Penkowa M, Tio L, Giralt M, Quintana A, Molinero A, Atrian S, Vasak M, Hidalgo J (2006) Specificity and divergence in the neurobiological effects of different metallothioneines after brain injury. Neurosci Res 83:974–984

Persellin RH, Ziff M (1966) The effect of gold salt on lysosomal enzymes of the peritoneal macrophage. Arthritis Rheum 9:57–65

Potashkin JA, Meredith GE (2006) The role of oxidative stress in the dysregulation of gene expression and protein metabolism in neurodegenerative disease. Antoxid Redox Signal 8:144–151

Roach P, Eglin D, Rohde K, Perry CC (2007) Modern biomaterials: a review—bulk properties and implications of surface modifications. J Mater Sci Mater Med 18:1263–1277

Santos E, Monzon-Mayor M, Romero-Alemán MM, Yanes C (2008) Distribution of Neurotrophin-3 during the ontogeny and regeneration of the lizard (gallotia gallot) visual system. Dev Neurobiol 68:31–44

Seifert G, Schilling K, Steinhauser C (2006) Astrocyte dysfunction in neurological disorders: a molecular perspective. Nat Rev Neurosci 7:194–206

Sennerby L, Thomsen P, Ericson LE (1993) Early tissue response to titanium implants inserted in rabbit cortical bone. J Mater Sci Mater Med 4:494–502

Sharma RP, McQueen EG (1981) Effects of gold sodium thiomalate on cytosolic copper and zinc in the rat kidney and liver tissues. Clin Exp Pharmacol Physiol 8:591–599

Simard AR, Rivest S (2004) Role of inflammation in the neurobiology of stem cells. NeuroReport 15:2305–2310

Sofroniew MV (2005) Reaktive astrocytes in neural repair and protection. Neuroscientist 11:400–407

Tozman EC, Gottlieb NL (1987) Adverse reactions with oral and parenteral gold preparations. Med Toxicol 2:177–189

Turrin NP, Rivest S (2006) Molecular and cellular immune models of neuroprotection. Mol Neurobiol 34:221–242

Vaccarino FM, Fagel DM, Ganat Y, Maragnoli ME, Ment LR, Ohkubu Y, Schwartz ML, Silbereis J, Smith KM (2007) Astroglial cells in development regeneration and repair. Neuroscientist 13:173–185

Van Raay TJ, Wang YK, Stark MR, Rasmussen JT, Francke U, Vetter ML, Rao MS (2001) frizzled-9 is expressed in neural precursor cells in the developing neural tube. Dev Genes Evol 211:453–457

Walton NM, Sutter BM, Laywell ED, Levkoff LH, Kearns SM, Marshall GP 2nd, Scheffler B, Steindler DA (2006) Microglia instruct subventricular zone neurogenesis. Glia 54:815–825

Yanni G, Nabil M, Farahat MR, Poston RN, Panayi GS (1994) Intramuscular gold decreases cytokine expression and macrophage numbers in the rheumatoid synovial membrane. Ann Rheum Dis 53:315–322

Zhang RL, Zhang ZG, Chopp M (2005) Neurogenesis in the adult ischemic brain: generation, migration, survival, and restorative therapy. Neuroscientist 11:408–416